The Characterization of Textures of Thin Films by Electron Diffraction

Bin Lu, Li Tang*, David N. Lambeth**, and David E. Laughlin

Department of Materials Science and Engineering
** Department of Electrical and Computer Engineering
Carnegie Mellon University, Pittsburgh, Pennsylvania 15213
* IBM Storage System Division, San Jose, CA 95193

Abstract

The distribution of intensity in reciprocal space of thin film with various textures is studied by means of a crystallographic analysis. Electron diffraction patterns of textured thin films are characterized in light of this analysis. Distinct angles and multiplicity factors of the reciprocal lattice rings are determined for bcc-Cr and hcp-Co thin films of the textures that are usually developed in thin films used for magnetic recording media. The intensity ratios of 0°-tilted electron diffraction pattern are also calculated and presented in tabular form. The texture axis distribution angle of a thin film can be determined by observing the presence or absence of rings of a 0°-tilted pattern or by studying the evolution of the arcs in the pattern with the tilt angles. The results of our studies of [112], [002] textured Cr thin films and the $(10\bar{1}0)$, $(11\bar{2}0)$ textured Co thin films by the electron diffraction technique are presented and discussed in terms of the analysis.

Grain Growth in Polycrystalline Materials III
Edited by H. Weiland, B.L. Adams,
and A.D. Rollett
The Minerals, Metals & Materials Society, 1998

1. Introduction

A polycrystalline thin film is usually produced when a material is sputter deposited onto a substrate. The orientations of the grains of the thin film are not usually random. Two types of preferred orientations (POs) are commonly observed, namely a lamella type and a fibrous type of texture[1]. In lamella texture, the crystalline grains of the thin film have same crystallogrphic plane parallel to a reference plane (usually the plane of the thin film). In fibrous texture, those individual grains have a particular crystallographic direction parallel to a reference direction (usually the normal of the thin film).

Most knowledge of crystallographic texture is based on bulk materials[2], which can readily be investigated by X-ray diffraction (XRD) techniques[3]. Since thin films are often only 10-100 nm thick with the grain sizes on the order of 10-20 nm, it is extremely difficult to obtain reliable diffracted intensities by XRD process. Moreover due to overlapping of diffraction peaks from the substrate and various layers of multilayered thin films, it is also very difficult to separate their diffraction effects. Electrons are scattered more strongly by atoms than x-rays[1]. Also TEM specimens can be prepared in such a way that electron diffraction (ED) can be carried out on any of the layers in a multilayered thin film.

Due to the extensive research on the minerals by ED in the past, comprehensive studies have been carried out both theoretically and experimently to determine the texture axis of a thin crystal of any Bravais lattice[4-6]. However, since many of the physical properties of thin films are strongly influenced by the quality of the texture, it is also important to know how good the texture is in addition to what kind of the texture is present. To the best of our knowledge, there has not been much published on the systematic and quantitative determination of the degree of a certain texture present in thin film[7].

In this paper, a unified treatment of the analysis of fibrous and lamellar textured thin films is presented based on crystallographic calculations and ED technique. Since the magnetic properties of Co-alloy thin films for longitudinal magnetic recording are strongly influenced by the preferred orientation of the easy magnetization axis, the degree of texture in these thin films is an important parameter which determines the performance of the media. Results from the crystallographic analysis and actual ED patterns of these kinds of textured thin films will be presented.

2. Reciprocal Lattice

In the case of lamellar textures, the grains of the film have the same crystallographic planes (h'k'l') parallel to the film surface with their in-plane directions arranged randomly. The fibrous texture has a common direction [uvw] of the grains aligned normal to the surface of the film and other in-plane directions arranged randomly. Accordingly, the reciprocal lattice of the textures are similar to that of a single crystal with all of the reciprocal-lattice nodes rotated around the surface normal of the thin film. Hence, (hkl) reciprocal-lattice nodes become (hkl) reciprocal-lattice rings around the surface normal. For a family of {hkl} in which the lattice planes have same d-spacing (d_{hkl}) and structure factor, the corresponding reciprocal-lattice rings stay on the same reciprocal spherical shell but at different latitudes (see Fig. 1). The total number of the planes is the multiplicity (P) of the family. To simplify things, no distinction is made here between (hkl) and ($\bar{h}\bar{k}\bar{l}$). However, the number of the {hkl} rings is equal to N, where $N \leq P$, since some planes in the {hkl} family may have same distinct angle, η, with respect to texture axis.

Fig. 1 illustrates the reciprocal-lattice rings of {222} family in a bcc [112] textured thin film. The multiplicity P for {222} is 4. However, since the ($\bar{2}22$) ($2\bar{2}2$) rings have the same value of $\eta = 61.9°$, N equals to 3 in this case, i.e., there are only 3 rings on the reciprocal semi-shell. If the texture is not ideal, i.e., the texture axis is distributed about the surface normal in a solid angle with an angular interval α, the reciprocal-lattice rings become spherical belts

subtending an angle of 2α from the origin (Fig. 2). Therefore, α can be used as a parameter evaluating the quality of the texture.

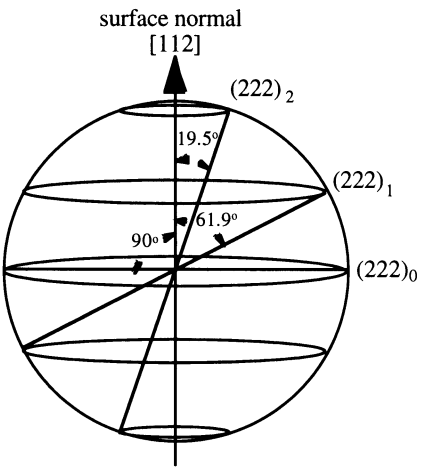

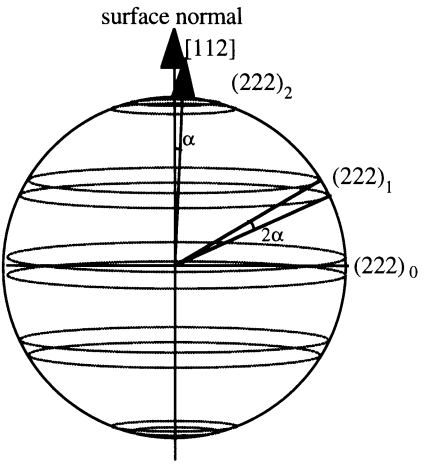

Fig.1 {222} rings of a [112] textured bcc film. **Fig.2** {222} belts of a [112] textured bcc film.

Tables 1-5 list the maximum possible number of distinct angles between any given crystallographic direction [uvw] (fibrous texture) or plane (h'k'l') (lamellar texture) and all planes in a given family in cubic, tetragonal, orthorhombic, hexagonal and monoclinic crystal systems. The monoclinic system is too trivial to list. Here, we let h < k < l, and u < v < w (h' <k' < l'). In these tables, the multiplicity (p) of each reciprocal-lattice rings is given in decreasing order of distinct angles. A "p" with an asterisk indicates the distinct angle of that ring is equal to 90°. For example, in the cubic system (Table 1), there are 8 distinct angles between a {0kl} plane family and the [0vw] direction (for fibrous texture) or the (0vw) plane (for lamella texture). The total multiplicity (P) of the {0kl} family is 12, but the multiplicities (p) of each distinct angles are 1, 1, 2, 2, 2, 2, 1, 1, lised in a descending order of the distinct angles. It will be shown below that these distinct angles are very useful for analysing the behaviour of the tilted electron diffraction patterns at particular tilting angles. The multiplicities (p) are required for calculating the intensities of the diffraction rings in a 0°-tilted EDP. It should be noted that Table 1-6 are calculated for the universal cases. For a particular crystal, the value of several distinct angles in a same plane family may be equal. Consequently, there will be less distinct angles and larger multiplicities (p).

3. Electron Diffraction Patterns

When the incident electron beam is parallel to the surface normal of the film, only those reciprocal-lattice rings with the angle of $\eta \geq 90° - \alpha$ will be present in the electron diffraction pattern (EDP). The local intensity ratio of these rings is given by[1]

$$\frac{I_{h_1k_1l_1}}{I_{h_2k_2l_2}} = \frac{\left|\Phi_{h_1k_1l_1}\right|^2 d^2_{h_1k_1l_1} p_1}{\left|\Phi_{h_2k_2l_2}\right|^2 d^2_{h_2k_2l_2} p_2} \tag{1}$$

where I_{hkl} is the local intensity of (hkl) diffraction ring, Φ_{hkl} the structure amplitude, p the multiplicity factor.

Table 1. Maximum number of distinct angles between any given direction (uvw)/plane (h'k'l') and a given plane family {hkl} in the cubic system.

Direction	uvw	uuw	0vw	110	111	001
plane	h'k'l'	h'h'l'	0k'l'	110	111	001
hkl(24)	24(1)	12(2)	12(2)	6(4)	4(6)	3(8)
hhl(12)	12(1)	7(1)	6(2)	4(2*)	3(3)	2(8)
		(2)		(4)	(6)	(4)
		(2)		(2)	(3)	
		(2)		(4)		
		(2)				
		(2)				
		(1)				
0kl(12)	12(1)	6(2)	8(1)	4(2)	2(6)	3(4*)
			(1)	(4)		(4)
			(2)	(4)		(4)
			(2)	(2)		
			(2)			
			(2)			
			(1)			
			(1)			
0kk(6)	6(1)	4(2)	4(1)	3(1)	2(3)	2(4)
		(1)	(2)	(4)	(3*)	(2*)
		(2)	(2)	(1*)		
		(1*)	(1)			
hhh(4)	4(1)	3(1)	2(2)	2(2)	2(1)	1(4)
		(2)	2(2)	(2*)	(3)	
		(1)				
00l(3)	3(1)	2(1)	3(1)	2(2)	1(3)	2(1)
		(2)	(1)	(1*)		(2*)
			(1*)			

Table 2. Maximum number of distinct angles between any given direction (uvw)/plane (h'k'l') and a given plane family {hkl} in the tetragonal system.

Direction	uvw	uuw	0vw	uv0	110	010	001
plane	h'k'l'	h'h'l'	0k'l'	h'k'0	110	010	001
hkl(8)	8(1)	4(2)	4(2)	4(2)	2(4)	2(4)	1(8)
hhl(4)	4(1)	3(1)	2(2)	2(2)	2(2)	1(4)	1(4)
		(2)			(2*)		
		(1)					
0kl(4)	4(1)	2(2)	3(1)	2(2)	1(4)	2(2)	1(4)
			(2)			(2*)	
			(1)				
hk0(4)	4(1)	2(2)	2(2)	4(1)	2(2)	2(2)	1(4*)
hh0(2)	2(1)	2(1)	1(2)	2(1)	2(1)	1(2)	1(2*)
		(1*)			(1*)		
0k0(2)	2(1)	1(2)	2(1)	2(1)	1(2)	2(1)	1(2*)
			(1*)			(1*)	
00l(1)	1(1)	1(1)	1(1)	1(1*)	1(1*)	1(1*)	1(1)

Table 3. Maximum number of distinct angles between any given direction (uvw)/plane (h'k'l') and a given plane family {hkl} in the orthorhombic system.

Direction	uvw	0vw	u0w	uv0	100	010	001
plane	h'k'l'	0k'l'	h'0l'	h'k'0	100	010	001
hkl(4)	4(1)	2(2)	2(2)	2(2)	1(4)	1(4)	1(4)
0kl(2)	2(1)	2(1)	1(2)	1(2)	1(2*)	1(2)	1(2)
h0l(2)	2(1)	1(2)	2(1)	1(2)	1(2)	1(2*)	1(2)
hk0(2)	2(1)	1(2)	1(2)	2(1)	1(2)	1(2)	1(2*)
h00(1)	1	1*	1	1	1	1*	1*
0k0(1)	1	1	1*	1	1*	1	1*
00l(1)	1	1	1	1*	1*	1*	1

Table 4. Maximum number of distinct angles between any given direction (uvw)/plane (h'k'l') and a given plane family {hkl} in the hexagonal system.

Direction	uv.w	uu.w	0v.w	uv.0	11.0	01.0	00.1
plane	h'k'.l'	h'h'.l'	0k'.l'	h'k'.0	11.0	01.0	00.1
hk.l(12)	12(1)	6(2)	6(2)	6(2)	3(4)	3(4)	1(12)
hh.l(6)	6(1)	4(1)	3(2)	3(2)	2(2)	2(4)	1(6)
		(2)			(4)	(2*)	
		(2)					
		(1)					
0k.l(6)	6(1)	3(2)	4(1)	3(2)	2(4)	2(2)	1(6)
			(2)		(2*)	(4)	
			(2)				
			(1)				
hk.0(6)	6(1)	3(2)	3(2)	6(1)	3(2)	3(2)	1(6*)
hh.0(3)	3(1)	2(1)	2(2)	3(1)	2(1)	2(2)	1(3*)
		(2)	(1*)		(2)	(1*)	
0k.0(3)	3(1)	2(2)	2(1)	3(1)	2(2)	2(1)	1(3*)
			(2)		(1*)	(2)	
		(1*)					
00.l(1)	1(1)	1(1)	1(1)	1(1*)	1(1*)	1(1*)	1(1)

Table 5. Maximum number of distinct angles between any given direction (uvw)/plane (h'k'l') and a given plane family {hkl} in the monoclinic system.

Direction	uvw	u0w	010
plane	h'k'l'	h'0l'	010
hkl (2)	2(1)	1(2)	1(2)
h0l (1)	1	1	1*
0k0 (1)	1	1*	1

When the surface normal is tilted away from the incident electron beam about an in-plane axis the EDPs no longer appear as uniform rings. Now they appear as arcs due to the intersection of the Ewald sphere with the inclined reciprocal spherical belts. The relationship between an arc and the tilt angle is[8]:

$$\sin(\omega_0/2) = \sin\alpha / \sin\beta,\ \beta \le \alpha \le 90^\circ \quad \text{(for a (hkl)}_0 \text{ arc)} \tag{2}$$

where ω_0 is the angle subtended by the $(hkl)_0$ arc, β the tilt angle. Also:

$$\cos(\omega_i/2) = \cos(\eta_i + \alpha) / \sin\beta,\ \ 90 - \eta_i - \alpha \le \beta \le 90 - \eta_i + \alpha \quad \text{(for a (hkl)}_i \text{ arc)} \tag{3}$$

where ω_i is the angle subtended by the $(hkl)_i$ arc, η_i the distinct angle. Thus, with the known tilt angle β and measured ω_0 or ω_i values, the value of α can be determined from the slope of the straight line of the $\sin(\omega_0/2)$ vs. $1/\sin\beta$ plot or the $\cos(\omega_i/2)$ vs. $1/\sin\beta$ plot.

4. Textured thin films of bcc-Cr and hcp-Co

Thin film media for longitudinal magnetic recording normally consists of a seed layer, an underlayer, and a magnetic layer, etc.[9]. These thin film layers are usually textured polycrystalline films orientated in such a way that the Co $(10\bar{1}0)$ or $(11\bar{2}0)$ texture can be obtained on the top. Previous studies[10] have shown that bcc structure of Cr can serve as a good underlayer for hcp Co-alloy layer. The orientation relationship between the underlayer and magnetic layer are: Co $(11\bar{2}0)$/Cr (200), and Co $(10\bar{1}0)$/Cr (112). Based on equation (1) the relative intensities of diffraction rings in a 0°-tilt EDP of a given texture of Cr (bcc) and Co (hcp) can be calculated. These values are listed in Tables 6 and 7 with the distinct angles and multiplicities (p) of a given {hkl} family.

Table 6. Distinct angles between a given texture axis and a given plane family in bcc Cr.

{hkl}(P)	110(6)	200(3)	211(12)	220(6)	310(12)	222(4)	321(24)	400(3)
d_{hkl}	2.039	1.444	1.177	1.020	0.912	0.833	0.771	0.722
$\sin\theta/\lambda$	0.245	0.347	0.425	0.490	0.548	0.600	0.648	0.693
f_{el}	2.899	2.049	1.660	1.361	1.155	1.014	0.894	0.792
F_{hkl}	5.778	4.098	3.320	2.722	2.310	2.028	1.788	1.584
$\mathbf{I}_{random}$	**100**	**13**	**22**	**6**	**6**	**1**	**6**	**0.4**
$\mathbf{I}_{[002]}$	**100**	**25**	**0**	**6**	**6**	**0**	**0**	**1**
Angles(p)	90(2) 45(4)	90(2) 0(1)	65.9(8) 35.3(4)	90(2) 45(4)	90(4) 71.6(4) 18.4(4)	54.7(4)	74.5(8) 57.7(8) 36.7(8)	90(2) 0(1)
$\mathbf{I}_{[112]}$	**100**	**0**	**0**	**6**	**0**	**2**	**3**	**0**
Angles(p)	90(1) 73.2(2) 54.7(1) 30(2)	65.9(2) 35.3(1)	80.4(4) 70.5(1) 60(2) 48.2(2) 33.6(2) 0(1)	90(1) 73.2(2) 54.7(1) 30(2)	82.6(2) 75.0(2) 58.9(2) 49.8(4) 25.4(2)	90(1) 61.9(2) 19.5(1)	90(2) 83.7(2) 77.4(2) 70.9(6) 57.0(2) 49.1(2) 40.2(4) 29.2(2) 10.9(2)	65.9(2) 35.3(1)

Table 7. Distinct angles between a given texture axis and a given plane family in hcp Co.

{hkl}	$10\underline{1}0$	0002	$10\underline{1}1$	$10\underline{1}2$	$11\underline{2}0$	$10\underline{1}3$	$20\underline{2}0$	$11\underline{2}2$	$20\underline{2}1$	0004	$20\underline{2}2$	$10\underline{1}4$
(P)	(3)	(1)	(6)	(6)	(3)	(6)	(3)	(6)	(6)	(1)	(6)	(6)
d_{hkl}	2.174	2.030	1.917	1.486	1.253	1.151	1.087	1.068	1.050	1.015	0.959	0.922
$\sin\theta/\lambda$	0.230	0.246	0.261	0.336	0.398	0.434	0.460	0.468	0.476	0.491	0.521	0.542
f_{el}	20.049	19.500	18.994	16.574	14.752	13.786	13.133	12.943	12.754	12.412	11.780	11.351
F_{hkl}	20.049	39.000	32.899	16.574	29.504	23.878	13.133	25.886	22.091	24.824	11.780	11.351
$\mathbf{I}_{random}$	**39**	**22**	**100**	**30**	**19**	**26**	**6**	**24**	**20**	**4**	**9**	**8**
$\mathbf{I}_{(10\underline{1}0)}$	**0**	**100**	**0**	**0**	**29**	**0**	**0**	**36**	**0**	**18**	**0**	**0**
Angles(p)	60(2)	90(1)	63.8(4)	70.0(4)	90(1)	74.6(4)	60(2)	90(2)	61.1(4)	90(1)	63.8(4)	77.8(4)
	0(1)		28.1(2)	46.9(2)	30(2)	58.0(2)	0(1)	42.5(4)	15.0(2)		28.1(2)	64.9(2)
$\mathbf{I}_{(11\underline{2}0)}$	**39**	**67**	**100**	**30**	**0**	**26**	**6**	**0**	**20**	**11**	**9**	**8**
Angles(p)	90(1)	90(1)	90(2)	90(2)	60(2)	90(2)	90(1)	64.8(4)	90(2)	90(1)	90(2)	90(2)
	30(2)		40.2(4)	53.7(4)	0(1)	62.7(4)	30(2)	31.7(2)	33.2(4)		40.2(4)	68.5(4)

For the purpose of comparison, the intensity ratios of the random oriented case is also listed in the tables. For example, in a Cr film with [112] texture (Table 6), the reciprocal-lattice rings, such as, (110), (220), (222), (321) which have a distinct angle of 90° are present in the EDP. While those rings, such as, (200), (112), (310), (400) should be missing, as there is no 90° distinct angle in their families. Their largest distinct angles are 65.9, 80.4, 82.6, and 65.9 degree respectively. However, it should be noted if the texture is not ideal (for example, one in which the distribution angle $\alpha \geq 9.6°$), the (112) and (310) rings will be present in the EDP.

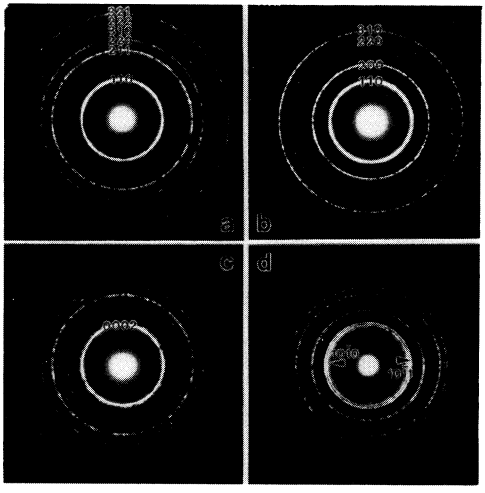

Fig.3. 0°-tilt EDPs of (a) [112] Cr, (b) [002] Cr, (c) $[10\bar{1}0]$ Co, and (d) $[11\bar{2}0]$ Co textured thin films.

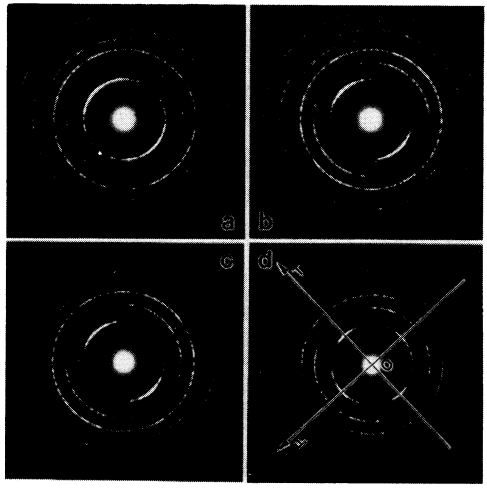

Fig.4. Tilted EDPs of [112] textured Cr thin film at (a) 22° (b) 32° (c) 42° (d) 52° with OT as the tilt axis.

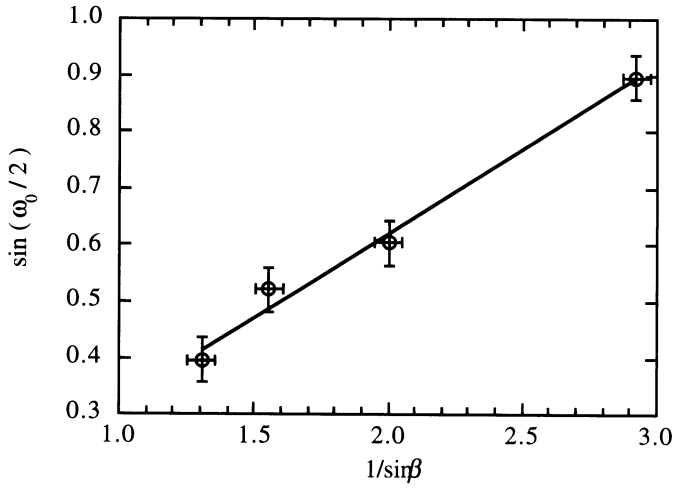

Fig. 5. Plot of $\sin(\omega_{110}/2)$ vs. $1/\sin\beta$ for the (110) ring of Fig. 4a-d.

Fig. 3a shows an EDP of [112] textured Cr thin film. The (200) ring is missing because the largest distinct angle in {200} family referred to [112] texture axis is 65.9° (Table 6), which is too far away from 90° for it to be present. The (112) ring is present because the largest distinct angle of the {112} family is 80.4°, which is closer to 90°. This suggests that the distribution angle of the texture axis is greater than 9.6° but less than 24.1°. Fig. 3b shows an EDP of [002] textured Cr film. The (112) and (222) rings are missing because their largest distinct angles (Table 6) are 65.9° and 54.7° respectively, which means that these rings are too far from 90°. The same reasoning holds for the (321) ring, whose distinct angle is 74.5° is also missing. Therefore the distribution angle of the Cr [002] texture axis is less than 15.5°.

Fig. 3c and d shows the 0°-tilted EDP of $[10\bar{1}0]$ and $[11\bar{2}0]$ textured Co film. One can easily tell the difference between the two patterns. The $(10\bar{1}0)$, $(10\bar{1}1)$, $(10\bar{1}\bar{2})$ rings are extremely weak in the $[10\bar{1}0]$ pattern, while the $(11\bar{2}0)$ and $(11\bar{2}2)$ rings are missing in the $[11\bar{2}0]$ pattern. This is consistent with Table 7.

Thus the texture of a thin film can be *qualitatively* studied by observing a 0°-tilted EDP and noting which ring is missing and by estimating relative intensities of those rings that are present.

Fig. 4a-d shows a tilting EDP series of the [112] textured Cr film corresponding to Fig. 3a. The 90°-ring $(110)_0$ splits into arcs when the tilt angle is 22° (Fig. 4a). At the same time, arcs of the first non-90°-ring $(002)_1$ appear. As the tilt angle increases the $(110)_0$ arcs become smaller, while the $(002)_1$ arcs become larger. At 42° (Fig. 4c) arcs of the second non-90°-ring $(110)_2$ whose distinct angle is 54.7° appear and they get bigger at a tilt of 52° (Fig. 4d). The reason that arcs of the first non-90°-ring $(110)_1$ with 73.2° angle does not appear is because it has merged with the 90° ring due to the distribution angle α of the texture axis.

Fig. 5 plots the relationship between $\sin(\omega_{110}/2)$ and $1/\sin\beta$ based on the $(110)_0$ arcs of the tilted EDPs of the Cr [112] texture in Fig. 4a-d. According to the equation (2), the distribution angle α of the [112] texture axis is determined as 10.2° from the slope of the plot.

This value is consistent with the above qualitative analysis of the 0°-tiled Cr [112] pattern (Fig. 3a).

5. Conclusions

From the reciprocal space analysis of fibrous and lamellar textured thin films, the maximum number of distinct angles and multiplicity (p) of each (hkl) ring in a {hkl} family can be deduced. It has been shown that the maximum number of distinct angles is the same in either fibrous texture or lamellar texture. Electron diffraction patterns consist of $(hkl)_0$ rings when the electron beam is parallel to the surface normal of the film. When the texture axis is tilted away from the incident electron beam around an in-plane axis, the EDP no longer consists of uniform rings but arcs. Based on the above analysis, the behaviour of each diffraction ring in a tilted EDP series can be predicted once the texture axis and its distribution angle (α) is known. On the other hand, if the texture axis is known, the distribution angle (α) can be quantitatively determined. Moreover, a qualitative estimation of the distribution angle can be obtained based on only the 0°-tilted pattern.

The distinct angles, multiplicity (p), and intensity ratios of diffraction rings for a 0°-tilted EDP are calculated for different textures of bcc-Cr and hcp-Co thin films. The texture axis distribution angle was determined by the study of both the 0°-tilted pattern and the evolution of the arcs with the tilt angles. [112], [002] textured Cr thin films, $[10\bar{1}0]$, $[11\bar{2}0]$ textured Co thin films are studied. And the texture axis distribution angle of the Cr [112] texture is determined to be 10.2°.

Acknowledgement

Some of the work included here was supported by the Data Storage System Center at Carnegie Mellon University, by the National Science Foundation EDC 89-07068. The government has certain rights to this material. Bin Lu was supported by a grant from INTEVAC.

References

[1] B. K. Vainshtein, Structure Analysis by Electron Diffraction, (New York, NY: Pergamon, 1964), 4, 70, 186.

[2] C. S. Barrett and T. B. Massalski, Structure of Metals, 3rd revised ed., (New York, NY: Pergamon, 1980), 193.

[3] B. D. Cullity, Elements of X-ray Diffraction, (Reading, MA: Addison Wesley, 1978), 295.

[4] B. B. Zvyagin, International Tables for Crystallography, Vol. C, Edited by A. J. C. Wilson, (Dordrecht: Kluwer Academic Publishers, 1992), 359.

[5] R. Ruhle, Optik , **7** (1950), 267-284.

[6] L. Reimer, Transmission Electron Microscopy, (Springer-Verlag, 1984), 407.

[7] L. Reimer, and K. Freking, Z. Phys., 184 (1965), 119-129

[8] L. Tang and D. E. Laughlin, "Electron Diffraction Patterns of Fibrous and Lamellar Textures Polycrystalline Thin films. I. Theory", J. Appl. Cryst., 29 (1996), 411-418.

[9] David E Laughlin, Y. C. Feng, David N. Lambeth, Li-Lien Lee, Li Tang, "Design and Crystallography of Multilayered Media", Journal of Magnetism and Magnetic Materials, 155 (1996), 146-150.

[10] K. Hono, B. Wong, and D. E. Laughlin, "Crystallography of Co/Cr bilayer magnetic thin films", J. Appl. Phys., 68 (1990), 4734-4740.